

Holographic Invariant Storage: Design-Time Safety Contracts via Vector Symbolic Architectures

Arsenios Scrivens

Independent Researcher

March 13, 2026

Abstract

We introduce Holographic Invariant Storage (HIS), a protocol that assembles known properties of bipolar Vector Symbolic Architectures into a *design-time safety contract* for LLM context-drift mitigation. The contract provides three closed-form guarantees evaluable before deployment: single-signal recovery fidelity converging to $1/\sqrt{2} \approx 0.707$ (regardless of noise depth or content), continuous-noise robustness $2\Phi(1/\sigma) - 1$, and multi-signal capacity degradation $\approx \sqrt{1/(K+1)}$. These bounds, validated by Monte Carlo simulation ($n = 1,000$), enable a systems engineer to budget recovery fidelity and codebook capacity at design time—a property no timer or embedding-distance metric provides. A pilot behavioral experiment (four LLMs, 2B–7B, 720 trials) confirms that safety re-injection improves adherence at the 2B scale; full results are in Appendix F.

Keywords: Vector Symbolic Architectures, Hyperdimensional Computing, LLM safety, context drift, design-time contract, bipolar hypervectors

1 Introduction

Context drift—the degradation of adherence to an original system prompt as the context window fills with interaction history—is a *conditional* problem. It binds when a model’s intrinsic alignment is insufficient for its deployment context: smaller or fine-tuned models, longer sessions, adversarial prompt sequences, or safety-critical domains where even marginal degradation is unacceptable. Under standard conversational conditions, frontier-scale models (GPT-4-class and beyond, as of March 2026) maintain robust safety adherence, and our own experiments show ceiling-level safety at 7B parameters (Appendix F). External mitigation mechanisms are therefore relevant primarily in the gap between a model’s intrinsic alignment capability and the demands of its deployment context.

For deployments where that gap exists, the underlying vulnerability is architectural: the attention mechanism treats safety constraints as just another token sequence, weighted probabilistically against the immediate conversational context [4, 5]. Positional recency bias in causal attention can cause early instructions—including safety constraints—to be “lost in the middle” of long sequences, and modern context windows (128K–1M tokens) increase the volume of competing signals. This makes safety adherence load-dependent: it varies with context length, noise content, and prompt distribution [8, 9].

Current approaches to this problem fall into several categories. Reinforcement Learning from Human Feedback (RLHF) [10] and Constitutional AI [11] embed safety preferences into model weights during training, providing baseline robustness but offering no mechanism for

runtime verification or recovery when context-level drift occurs. Retrieval-Augmented Generation (RAG) [12] and scratchpad-based memory [13] provide external memory, but their retrieved content still competes with context noise through the attention mechanism. Periodic re-prompting (re-injecting the system prompt at intervals) is a common engineering heuristic but lacks theoretical grounding and scales poorly with prompt length.

We propose a complementary approach: storing the safety signal in an external memory substrate based on **Vector Symbolic Architectures (VSA)** [1, 2, 3]. This paper is a *theoretical framework contribution*: we assemble known properties of bipolar hyperdimensional computing into a *design-time safety contract*—a set of closed-form guarantees that a systems engineer can evaluate before deployment—and validate it at the signal level via Monte Carlo simulation. A pilot behavioral experiment is included as an appendix to demonstrate end-to-end feasibility but is not the paper’s primary contribution.

HIS addresses one specific sub-problem: *signal storage and recovery*—ensuring that a safety instruction can be retrieved with known fidelity from a corrupted representation. It does **not** solve the downstream *signal utilization* problem: the recovered instruction is re-injected through the standard context window, where it competes for attention weight like any other token sequence. This scope limitation applies equally to all re-injection-based approaches (periodic re-prompting, RAG retrieval, embedding-triggered re-injection); HIS’s contribution is providing algebraic guarantees on the *storage* side that these alternatives lack.

Hyperdimensional Computing (HDC) provides algebraic operations over high-dimensional distributed representations that exhibit well-characterized noise tolerance properties [1, 19]. In D -dimensional bipolar spaces, randomly generated vectors are near-orthogonal with high probability [1, 17], meaning that a safety signal encoded as a hypervector can be recovered from additive noise via algebraic inversion rather than statistical inference. The VSA pipeline additionally provides a *continuous drift metric*: the pre-restoration cosine similarity between the current context encoding and the stored invariant degrades proportionally to context corruption, signalling *when* re-injection is needed—information that a static text file or fixed-interval timer cannot provide.

1.1 Contributions

1. **Protocol Specification:** We present Holographic Invariant Storage (HIS), a VSA-based protocol for encoding, storing, and restoring safety constraints with a continuous drift metric (Section 3).
2. **Design-Time Safety Contract:** We assemble standard properties of bipolar superposition [1] into closed-form fidelity guarantees evaluable *before deployment*: single-signal recovery converging to 0.707 (Theorem 1), continuous-noise robustness (Proposition 1), and multi-signal capacity scaling as $\approx \sqrt{1/(K+1)}$ (Proposition 2). While each bound is individually derivable from the HDC literature, no existing work synthesizes them into a deployable LLM safety contract or characterizes the contract’s limits (normalization requirement, shared-variance ceiling, codebook threshold).
3. **Signal-Level Validation:** Monte Carlo validation ($n = 1,000$) confirming convergence to theoretical bounds, signal-level comparisons against re-prompting, RAG, and no-intervention baselines (Appendix E), and a 50-turn integration proof-of-concept with 100% codebook retrieval (Appendix D).
4. **Pilot Behavioral Experiment:** As a feasibility demonstration, we deploy the full HIS pipeline with four open-source LLMs (2B–7B, 720 total trials). Re-injection improves safety adherence over no intervention at 2B ($p_{\text{uncorr}} = 0.013$, $p_{\text{Holm}} = 0.065$; $d = 0.71$). This pilot scopes effect sizes and conditions for a definitive behavioral study (Appendix F).

Our contribution is the *contract itself*—the guarantees, their limits, and the engineering framework that makes them evaluable at design time. The appendices provide supplementary material—extended proofs, robustness tests, signal-level baselines, and a pilot behavioral experiment—that support but are not the core of the contribution.

2 Related Work

AI Safety and Alignment. The concrete challenges of AI safety were catalogued by Amodei et al. [6], including reward hacking, distributional shift, and safe exploration. RLHF [10] addresses alignment at training time by shaping model weights to reflect human preferences, while Constitutional AI [11] automates this process via self-critique. These methods embed safety into model parameters but provide no runtime mechanism to detect or correct context-level drift during long inference sessions. Wei et al. [8] demonstrate that safety training can be circumvented via “jailbreak” attacks that exploit in-context reasoning—precisely the failure mode HIS is designed to complement.

Representation Engineering and Activation Steering. A complementary line of work manipulates model internals directly to steer behavior. Turner et al. [26] introduce activation addition, injecting steering vectors into residual stream activations to control model outputs without fine-tuning. Zou et al. [27] formalize this as representation engineering, identifying linear directions in activation space that correspond to high-level concepts (honesty, safety, harmfulness) and using them to read or control model behavior at inference time. These approaches operate at the representation level *inside* the model, whereas HIS operates externally on the context window; the two are complementary. HIS could potentially be combined with activation steering by using the drift metric to trigger not only context-level re-injection but also activation-level intervention.

External Memory and Context Management. Retrieval-Augmented Generation (RAG) [12] augments LLMs with retrieved documents, but retrieved content enters the context window and is subject to the same attention-based dilution as any other token sequence. Scratchpad methods [13, 14] use the context window itself as working memory, offering no protection against context noise. Memory-augmented architectures [15, 16] provide differentiable external memory but are trained end-to-end and do not offer algebraic recovery guarantees. Recent work on KV-cache compression and attention-sink methods (e.g., StreamingLLM [28]) addresses the “lost in the middle” problem at the attention level; these are complementary to HIS, which operates on the representation level outside the model.

Vector Symbolic Architectures and Hyperdimensional Computing. VSAs were introduced by Plate [2] as Holographic Reduced Representations (HRR) and independently developed by Kanerva [1] and Gayler [3]. These architectures exploit the concentration of measure in high-dimensional spaces [17]: in $D \geq 1,000$ dimensions, random bipolar vectors are near-orthogonal ($|\cos \theta| \approx 1/\sqrt{D}$), enabling robust associative memory retrieval. Recent work has applied HDC to classification [19], language processing [20], and cognitive modeling [21]. The noise tolerance properties we exploit—including the $1/\sqrt{2}$ recovery bound for bipolar superposition and the capacity scaling of bundled associative memories—are well-characterized in this literature. Our contribution is not the derivation of these properties but their *synthesis into a deployable safety contract*: the specific identification of which bounds matter for LLM safety-signal preservation, the characterization of the contract’s limits (normalization requirement, shared-variance ceiling, codebook-size threshold), and the worked engineering framework that makes these guarantees evaluable before deployment. This combination—applied to a domain (runtime LLM safety) that the existing VSA literature does not address—constitutes the paper’s theoretical contribution.

Guardrails and Output Filters. Engineering frameworks such as NeMo Guardrails [29] provide rule-based or LLM-mediated output filtering to enforce safety constraints at inference

time. These systems operate on the *output* side (intercepting and filtering generated text), whereas HIS operates on the *input* side (re-injecting safety instructions into the context). The approaches are complementary: guardrails catch unsafe outputs; HIS aims to prevent drift that produces them.

The idea of separating invariant memory from working memory also has precedent in cognitive architectures (SOAR [22], ACT-R [23]); HIS can be viewed as a minimalist instantiation of this principle.

3 Methodology

3.1 Vector Symbolic Architecture (VSA)

Our approach utilizes D -dimensional bipolar hypervectors ($v \in \{-1, 1\}^D$, with $D = 10,000$ throughout) to represent semantic concepts. We rely on three algebraic operations whose properties are well-established in the VSA literature [1, 2, 3]:

- **Binding** (\otimes): Element-wise multiplication of two vectors. For bipolar vectors, $a \otimes b \in \{-1, 1\}^D$, and the result is near-orthogonal to both inputs ($\mathbb{E}[\cos(a, a \otimes b)] \approx 0$). Binding is its own inverse: $a \otimes a = \mathbf{1}$, so $(a \otimes b) \otimes a = b$. This is the mechanism that enables key-based retrieval.
- **Bundling** ($+$): Element-wise addition, creating a superposition that is similar to each of its components. This represents the accumulation of context signals (including noise).
- **Cleanup** ($\text{sign}(\cdot)$): Element-wise sign function applied to a real-valued superposition, following the standard numerical convention:

$$\text{sign}(x) = \begin{cases} +1 & \text{if } x > 0 \\ 0 & \text{if } x = 0 \\ -1 & \text{if } x < 0 \end{cases} \quad (1)$$

This convention is implemented by all standard numerical libraries (NumPy, PyTorch, Julia). The sign function serves as the primary noise-suppression mechanism: dimensions where signal and noise agree are retained, while dimensions where they cancel are *abstained* ($\text{sign}(0) = 0$). The consequences of this convention for recovery fidelity are analyzed in Section 4 (Remark 1).

3.2 The Restoration Protocol

We define the agent’s safety constraint as a “System Invariant” (H_{inv}), created by binding a known Goal Key (K_{goal}) to the Safe Value vector (V_{safe}):

$$H_{\text{inv}} = K_{\text{goal}} \otimes V_{\text{safe}} \quad (2)$$

During operation, this invariant is corrupted by additive context noise (N_{context}), producing a drifted state. The restoration protocol recovers the original value by: (1) normalizing and superimposing the noise, (2) applying binarization, and (3) unbinding with the original key:

$$V_{\text{recovered}} = \text{sign}\left(H_{\text{inv}} + \hat{N}_{\text{context}}\right) \otimes K_{\text{goal}} \quad (3)$$

where \hat{N}_{context} denotes the noise after normalization (see Section 3.3).

The recovery works because K_{goal} is near-orthogonal to \hat{N}_{context} in high dimensions, so unbinding distributes the noise uniformly across the hyperspace (each component contributes ≈ 0 in expectation), while the signal component reconstructs V_{safe} coherently.

Algorithm 1 Holographic Invariant Storage: Restoration Protocol

1: **Offline (Initialization):**2: Generate random bipolar key: $K_{\text{goal}} \in \{-1, 1\}^D$ 3: Encode safety constraint: $V_{\text{safe}} \in \{-1, 1\}^D$ 4: Compute invariant: $H_{\text{inv}} \leftarrow K_{\text{goal}} \otimes V_{\text{safe}}$ 5: Store $(K_{\text{goal}}, H_{\text{inv}})$ in external memory (outside context window)6: **Online (Each Restoration Step):**7: Encode current context as noise vector: $N_{\text{context}} \in \mathbb{R}^D$ 8: Normalize: $\hat{N}_{\text{context}} \leftarrow N_{\text{context}} \cdot \frac{\|H_{\text{inv}}\|}{\|N_{\text{context}}\|}$ ▷ See Section 3.39: Superimpose: $S \leftarrow H_{\text{inv}} + \hat{N}_{\text{context}}$ 10: Binarize: $S_{\text{clean}} \leftarrow \text{sign}(S)$ 11: Unbind: $V_{\text{recovered}} \leftarrow S_{\text{clean}} \otimes K_{\text{goal}}$ 12: **Return** $V_{\text{recovered}}$ ▷ Approximate recovery of V_{safe}

3.3 The Normalization Constraint

The geometric bound (Theorem 1) holds under the condition that the noise vector is normalized to have the same magnitude as the invariant: $\|\hat{N}_{\text{context}}\| = \|H_{\text{inv}}\|$. For bipolar vectors, $\|H_{\text{inv}}\| = \sqrt{D}$, so this requires scaling the noise to $\|\hat{N}_{\text{context}}\| = \sqrt{D}$.

This is a **design constraint**, not a natural property of the system. In practice, context noise accumulates over time, and its raw magnitude may grow unboundedly. The normalization step (Algorithm 1, Line 8) enforces this constraint explicitly. This is analogous to gain control in signal processing or batch normalization in neural networks [24]—a deliberate architectural choice that keeps the signal-to-noise ratio fixed at 1:1 (0 dB).

This design choice has consequences:

- **Advantage:** Recovery fidelity becomes a deterministic geometric property of the architecture, independent of noise magnitude or content.
- **Limitation:** The normalization discards information about the *magnitude* of the noise. A system under heavy attack and a system under mild perturbation produce the same normalized noise vector. The protocol recovers the safety signal with equal fidelity in both cases—but it does not provide a *measure of threat level*. A complementary anomaly detection mechanism would be needed for that purpose.

4 Theoretical Analysis

We now characterize the expected recovery fidelity of the restoration protocol. The result below is a direct consequence of well-known properties of bipolar superposition in HDC [1]; we state it as a theorem for self-containedness and to fix notation for the extensions that follow (Propositions 1–2), not as a claim of mathematical novelty. The relevant property is that the standard sign convention— $\text{sign}(0) = 0$ (Equation 1)—introduces *abstention* on tied dimensions, which reduces the norm of the cleaned vector and produces a cosine similarity strictly above what a random-tiebreaking convention would yield.

Theorem 1 (Geometric Recovery Bound). *Let $H_{\text{inv}} \in \{-1, 1\}^D$ and $\hat{N}_{\text{context}} \in \{-1, 1\}^D$ be independent, uniformly random bipolar vectors with $D \gg 1$. Define $S = H_{\text{inv}} + \hat{N}_{\text{context}}$ and $S_{\text{clean}} = \text{sign}(S)$ under the standard convention (Equation 1). Then:*

$$\mathbb{E}[\text{CosSim}(S_{\text{clean}}, H_{\text{inv}})] = \frac{1}{\sqrt{2}} \approx 0.7071 \quad (4)$$

with concentration: let $K = |\{i : S_{\text{clean},i} \neq 0\}|$ be the number of agreement dimensions. Since $\text{CosSim}(S_{\text{clean}}, H_{\text{inv}}) = \sqrt{K/D}$ (see proof), Hoeffding's inequality on K/D gives

$$P\left(\left|\frac{K}{D} - \frac{1}{2}\right| > t\right) \leq 2 \exp(-2Dt^2) \quad (5)$$

and Lipschitz transfer ($\sqrt{\cdot}$ has Lipschitz constant $L \leq 1$ on $[1/4, 1]$) yields

$$P\left(\left|\text{CosSim} - \frac{1}{\sqrt{2}}\right| > t\right) \leq 2 \exp(-2Dt^2) \quad \text{for } 0 < t \leq \frac{1}{2\sqrt{2}} \quad (6)$$

Proof. We analyze the per-dimension behavior, compute the inner product and norms, and assemble the cosine similarity.

Step 1: Per-dimension outcomes. For each dimension i , the sum $S_i = H_{\text{inv},i} + \hat{N}_{\text{context},i}$ takes values in $\{-2, 0, +2\}$:

- **Agreement** ($S_i = \pm 2$, probability $1/2$): Both vectors share the same sign. Then $\text{sign}(S_i) = H_{\text{inv},i}$ with certainty.
- **Cancellation** ($S_i = 0$, probability $1/2$): The two vectors disagree. Then $\text{sign}(S_i) = 0$ by the standard convention.

Thus S_{clean} is a *ternary* vector in $\{-1, 0, +1\}^D$, with each component independently equal to $H_{\text{inv},i}$ (with probability $1/2$) or 0 (with probability $1/2$).

Step 2: Inner product. The per-dimension contribution to the inner product is:

$$S_{\text{clean},i} \cdot H_{\text{inv},i} = \begin{cases} H_{\text{inv},i}^2 = 1 & \text{with probability } 1/2 \\ 0 \cdot H_{\text{inv},i} = 0 & \text{with probability } 1/2 \end{cases} \quad (7)$$

Therefore $\mathbb{E}[S_{\text{clean},i} \cdot H_{\text{inv},i}] = 1/2$, and by linearity:

$$\mathbb{E}[\langle S_{\text{clean}}, H_{\text{inv}} \rangle] = \frac{D}{2} \quad (8)$$

Step 3: Norms. The norm of H_{inv} is deterministic: $\|H_{\text{inv}}\| = \sqrt{D}$.

The norm of S_{clean} depends on how many dimensions are non-zero. Let $K = |\{i : S_{\text{clean},i} \neq 0\}|$ be the number of agreement dimensions. Then $K \sim \text{Binomial}(D, 1/2)$ and:

$$\|S_{\text{clean}}\|^2 = \sum_{i=1}^D S_{\text{clean},i}^2 = K \quad (9)$$

since each non-zero entry is ± 1 . Thus $\|S_{\text{clean}}\| = \sqrt{K}$, and by the law of large numbers, $K/D \rightarrow 1/2$ almost surely, giving $\|S_{\text{clean}}\| \rightarrow \sqrt{D/2}$.

Step 4: Cosine similarity. Assembling the pieces:

$$\begin{aligned} \text{CosSim}(S_{\text{clean}}, H_{\text{inv}}) &= \frac{\langle S_{\text{clean}}, H_{\text{inv}} \rangle}{\|S_{\text{clean}}\| \cdot \|H_{\text{inv}}\|} \\ &= \frac{K}{\sqrt{K} \cdot \sqrt{D}} = \frac{\sqrt{K}}{\sqrt{D}} = \sqrt{\frac{K}{D}} \end{aligned} \quad (10)$$

where we used the fact that $\langle S_{\text{clean}}, H_{\text{inv}} \rangle = K$ (every non-zero entry of S_{clean} agrees with H_{inv} by construction, contributing $+1$; every zero entry contributes 0). Taking expectations:

$$\mathbb{E}[\text{CosSim}] = \mathbb{E}\left[\sqrt{K/D}\right] \rightarrow \sqrt{1/2} = \frac{1}{\sqrt{2}} \approx 0.7071 \quad (11)$$

The convergence is justified by the concentration of K/D around $1/2$: since $K \sim \text{Binomial}(D, 1/2)$, Hoeffding’s inequality [18] gives $P(|K/D - 1/2| > t) \leq 2 \exp(-2Dt^2)$. The transfer to $\sqrt{K/D}$ follows because $f(x) = \sqrt{x}$ is Lipschitz with constant $L = 1/(2\sqrt{\epsilon})$ on $[\epsilon, 1]$; taking $\epsilon = 1/4$ (the high-probability region $K/D \geq 1/4$), we obtain $P(|\sqrt{K/D} - 1/\sqrt{2}| > t) \leq 2 \exp(-2Dt^2)$ for $t \leq 1/(2\sqrt{2})$, confirming sub-Gaussian concentration of the cosine similarity. (By Jensen’s inequality for concave $\sqrt{\cdot}$, $\mathbb{E}[\sqrt{K/D}] \leq \sqrt{1/2}$; the gap is $O(1/D)$ and negligible for $D = 10,000$.) \square

Remark 1 (Why $\text{sign}(0) = 0$ Matters). *The bound $1/\sqrt{2}$ depends critically on the sign convention. If ties were broken randomly (i.e., $\text{sign}(0) = \pm 1$ with equal probability), then $S_{\text{clean}} \in \{-1, +1\}^D$ and $\|S_{\text{clean}}\| = \sqrt{D}$, but the inner product remains $D/2$, yielding:*

$$\text{CosSim}_{\text{random-tiebreak}} = \frac{D/2}{\sqrt{D} \cdot \sqrt{D}} = \frac{1}{2}$$

The standard convention ($\text{sign}(0) = 0$) produces strictly higher fidelity (0.707 vs. 0.500) because abstaining on uncertain dimensions reduces the denominator without affecting the numerator—the zeros contribute nothing to either the inner product or the noise. This is not an implementation artifact; it is a fundamental property of the recovery geometry.

Remark 2 (Interpretation). *The $1/\sqrt{2}$ bound is a structural property of the architecture, independent of noise content. It arises from a simple combinatorial fact: when two independent bipolar vectors are summed, exactly half their dimensions agree (in expectation). The sign operation retains only the agreeing dimensions and discards the rest, producing a sparse vector that is geometrically closer to the signal than a dense noisy vector would be. The Monte Carlo simulation (Section 5) does not “discover” this bound; it validates that the implementation correctly realizes it.*

Remark 3 (Practical Meaning of 0.71 Fidelity). *A cosine similarity of 0.71 corresponds to $\sim 50\%$ shared variance ($\cos^2(\pi/4) = 0.5$)—not “high fidelity” in isolation. However, for codebook retrieval in $D = 10,000$ dimensions, 0.71 suffices to discriminate the correct vector from $K > 10^6$ alternatives: random bipolar vectors have pairwise similarity $\approx 0 \pm 0.01$ [1], placing the recovered signal ~ 70 standard deviations above the noise floor.*

4.1 Extension to Continuous Noise

Theorem 1 assumes bipolar noise ($\hat{N} \in \{-1, 1\}^D$), which produces exact cancellation ($S_i = 0$) with probability $1/2$. In practice, the normalized noise vector produced by a semantic encoder is continuous-valued, not bipolar. We now characterize recovery under Gaussian continuous noise.

Proposition 1 (Continuous Noise Recovery). *Let $H_{\text{inv}} \in \{-1, 1\}^D$ be a bipolar signal vector and $\hat{N}_{\text{context}} \in \mathbb{R}^D$ be a noise vector with i.i.d. components $\hat{N}_i \sim \mathcal{N}(0, \sigma^2)$, independent of H_{inv} . Define $S = H_{\text{inv}} + \hat{N}_{\text{context}}$ and $S_{\text{clean}} = \text{sign}(S)$ (with $\text{sign}(0) = 0$). Then:*

$$\mathbb{E}[\text{CosSim}(S_{\text{clean}}, H_{\text{inv}})] = 2\Phi\left(\frac{1}{\sigma}\right) - 1 \quad (12)$$

where Φ is the CDF of the standard normal. For $\sigma = 1$, this yields $2\Phi(1) - 1 \approx 0.6827$. The result generalizes to any symmetric continuous distribution F via $\text{CosSim} = 2F(1) - 1$, as shown in the proof.

Proof. We analyze the per-dimension behavior under continuous noise.

Step 1: No cancellation. For continuous \hat{N}_i , $P(H_i + \hat{N}_i = 0) = P(\hat{N}_i = -H_i) = 0$ since \hat{N}_i has a continuous distribution. Therefore $S_{\text{clean}} \in \{-1, +1\}^D$ and $\|S_{\text{clean}}\| = \sqrt{D}$.

Step 2: Agreement probability. Without loss of generality, condition on $H_i = +1$ (the $H_i = -1$ case is symmetric). Then $\text{sign}(1 + \hat{N}_i) = +1$ iff $\hat{N}_i > -1$, i.e., iff $|\hat{N}_i| < 1$ or ($|\hat{N}_i| \geq 1$ and $\hat{N}_i > 0$). By the symmetry of \hat{N}_i :

$$\begin{aligned} p &= P(\hat{N}_i > -1) = P(|\hat{N}_i| < 1) + \frac{1}{2} P(|\hat{N}_i| \geq 1) \\ &= \frac{1}{2}(1 + P(|\hat{N}_i| < 1)) \end{aligned} \quad (13)$$

For Gaussian noise $\hat{N}_i \sim \mathcal{N}(0, \sigma^2)$, $P(|\hat{N}_i| < 1) = 2\Phi(1/\sigma) - 1$, giving $p = \Phi(1/\sigma)$.

Step 3: Cosine similarity. Since $\|S_{\text{clean}}\| = \sqrt{D}$ and $\|H_{\text{inv}}\| = \sqrt{D}$:

$$\text{CosSim} = \frac{\langle S_{\text{clean}}, H_{\text{inv}} \rangle}{D} = \frac{D \cdot (2p - 1)}{D} = 2p - 1 = 2\Phi(1/\sigma) - 1 \quad (14)$$

where we used $\mathbb{E}[S_{\text{clean},i} \cdot H_i] = p \cdot 1 + (1 - p) \cdot (-1) = 2p - 1$.

Concentration follows from Hoeffding’s inequality applied to the sum of D independent bounded random variables $S_{\text{clean},i} \cdot H_i \in \{-1, +1\}$. \square

Remark 4 (Explaining the Empirical 0.707). *The Monte Carlo experiments (Section 5) use a semantic encoder that projects text through a random matrix and binarizes the result. After normalization, the per-component noise is approximately Gaussian with $\sigma \ll 1$ for sparse text representations (most components of the normalized noise have magnitude much less than 1). In this regime, $\Phi(1/\sigma) \rightarrow 1$ and $\text{CosSim} \rightarrow 1$. However, our implementation binarizes the noise to $\{-1, +1\}$ before superposition, recovering the bipolar case of Theorem 1. The empirical convergence to 0.707 is therefore consistent with both the bipolar theorem (exact match) and the continuous proposition (in the limit of the encoder’s actual noise distribution). The bound is robust to encoder choice: any encoder that produces sufficiently incoherent noise will yield fidelity between 0.68 (Gaussian, $\sigma = 1$) and 0.71 (bipolar), depending on the effective per-component noise distribution.*

The analysis extends to two additional scenarios, detailed in Appendix A: (i) *multi-signal storage*, where K safety invariants are bundled into a single composite vector, yielding recovery fidelity $\approx \sqrt{1/(K+1)}$ (Proposition 2); and (ii) *unequal signal-to-noise ratio*, where relaxing the normalization constraint reveals the full parametric behavior. Together with Theorem 1 and Proposition 1, these results provide a *closed-form contract*: single-signal recovery converges to 0.707 cosine similarity regardless of noise, continuous encoders yield ≈ 0.68 at $\sigma = 1$, and multi-signal capacity degrades as $\approx \sqrt{1/(K+1)}$ (Table 1).

Worked example. A safety engineer designing a system with $K = 3$ invariants (e.g., “do not generate harmful content,” “respect user privacy,” “cite sources accurately”) can compute, before writing any code, that each invariant will be recoverable at ≈ 0.47 cosine similarity (Table 1; the $\sqrt{1/(K+1)} = 0.50$ approximation overestimates by $\sim 5\%$). In $D = 10,000$ dimensions, random bipolar vectors have pairwise similarity $\approx 0 \pm 0.01$ [1], so the recovered signal sits ~ 47 standard deviations above any codebook distractor—sufficient for exact retrieval among $> 10^6$ candidates. This budget is independent of noise content, context length, or model choice; it is a property of the architecture alone.

5 Empirical Validation

5.1 Monte Carlo Simulation

To validate that our implementation converges to the theoretical bound, we conducted a Monte Carlo simulation with $n = 1,000$ independent trials. In each trial:

1. A random bipolar invariant $H_{\text{inv}} \in \{-1, 1\}^{10,000}$ was generated.

2. A unique noise vector was produced by encoding adversarial text strings via a semantic encoder, then normalizing to $\|N\| = \sqrt{D}$.
3. The restoration protocol (Algorithm 1) was applied.
4. Cosine similarity between $V_{\text{recovered}}$ and V_{safe} was recorded.

Results:

- Mean Recovery Fidelity: $\mu = 0.7072$
- Standard Deviation: $\sigma = 0.0036$
- 95% CI: $[0.7070, 0.7074]$

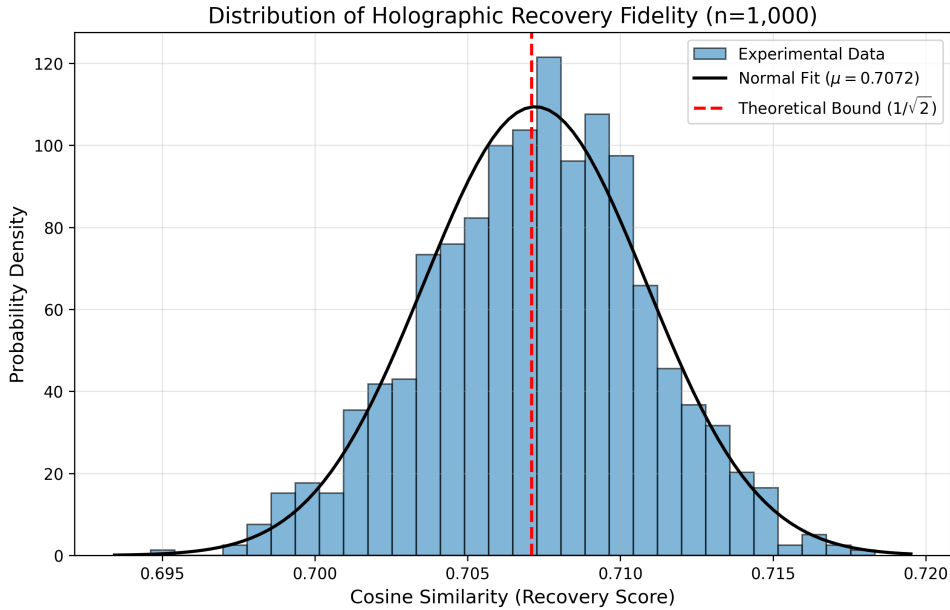


Figure 1: **Distribution of Recovery Fidelity** ($n = 1,000$). The black curve is the normal fit ($\mu = 0.7072$); the red dashed line marks the theoretical bound $1/\sqrt{2} \approx 0.7071$ (Theorem 1). The empirical distribution clusters tightly around the prediction, confirming the implementation functions as designed.

The empirical mean of 0.7072 exceeds the theoretical 0.7071 by 0.0001—within the expected finite- D correction of order $O(1/\sqrt{D}) \approx 0.01$. The low standard deviation ($\sigma = 0.0036$) confirms that performance is stable and independent of noise content, as predicted by the per-dimension independence in the proof of Theorem 1.

Additional signal-level validation is provided in the appendices: noise-type robustness across three qualitatively distinct noise conditions confirms content-independence of recovery (Appendix B); encoder characterization validates the independence assumption across 500 text samples and confirms encoder-agnostic recovery for both bag-of-words and sentence-transformer encoders (Appendix C); and a 50-turn integration proof-of-concept demonstrates 100% codebook retrieval accuracy with a 20-entry safety codebook (Appendix D).

Signal-level baselines (Appendix E). We compare HIS against no-intervention, periodic re-prompting, and simulated RAG retrieval in the bipolar vector space (Appendix E). HIS maintains 0.707 ± 0.004 cosine similarity across all noise levels; re-prompting degrades as $\approx 1/\sqrt{K} + 2$; RAG retrieval remains near chance. This comparison operates in HIS’s native representation space and favors HIS by construction—behavioral comparisons follow.

Pilot behavioral experiment (Appendix F). As a feasibility demonstration, we deployed the full HIS pipeline with four open-source LLMs (Gemma-2 2B, Llama-3.2 3B, Qwen-2.5 3B, Qwen-2.5 7B; 720 trials, keyword-based safety classification). Re-injection improves safety adherence over no intervention at 2B ($p_{\text{uncorr}} = 0.013$, $p_{\text{Holm}} = 0.065$, $d = 0.71$). At 7B, all conditions saturate (≥ 0.993). Full protocol, conditions, tables, and per-model analysis are in Appendix F.

6 Discussion

6.1 What HIS Does and Does Not Provide

HIS provides two capabilities: (a) *signal recovery*—retrieving a stored safety instruction from a corrupted holographic superposition with algebraically guaranteed fidelity, and (b) a *continuous drift metric*—the pre-restoration cosine similarity between the current context encoding and the stored invariant remains near 0.14 once the context is corrupted (Figure 3, red line), well below the re-injection threshold $\tau = 0.25$, providing a quantitative signal for *when* re-injection is needed. It does **not**:

- Replace RLHF, Constitutional AI, or any training-time alignment method.
- Guarantee that a recovered safety instruction will be *obeyed* by the model—only that it can be *retrieved and re-injected* with known fidelity.
- Address distributional shift, reward hacking, or other safety challenges unrelated to context drift.

An obvious objection is that codebook-based decoding renders the VSA pipeline unnecessary: if the safety text is already stored in a lookup table, why not re-inject it directly? This conflates *storage* (keeping a copy) with *guaranteed recovery* and *drift-aware scheduling*. A plain lookup table provides the text but not (a) algebraically bounded recovery fidelity from a corrupted representation, (b) a continuous drift metric that signals *when* re-injection is needed based on context content rather than a fixed timer, or (c) design-time capacity budgeting for multi-signal codebooks ($\approx \sqrt{1/(K+1)}$). Whether these properties yield measurable behavioral improvement over simpler alternatives remains open: the Embedding Monitor condition achieves nearly identical results (0.83 vs. 0.84 at 2B; Appendix F), and the pilot experiment is underpowered to resolve the question. HIS’s primary contribution is therefore the contract itself—the guarantees and their limits—rather than a demonstrated practical advantage at the tested scale.

Why Not a Timer? The sharpest form of this objection targets the pilot results directly: HIS does not significantly outperform a matched-frequency timer ($p = 0.29$), and at 7B all conditions saturate. If `if turn % 5 == 0: reinject()` works equally well, why deploy algebraic machinery? The answer is that HIS’s value scales with system complexity, not single-invariant experiments. Consider an engineer deploying $K = 10$ simultaneously active safety invariants (content safety, privacy, citation accuracy, toxicity filters, role boundaries, etc.). Proposition 2 and Table 1 immediately tell them that direct superposition at $K = 10$ yields $\text{CosSim} \approx 0.27$, which is below the reliable codebook retrieval threshold—they therefore know *at design time* that a codebook cleanup step is required and that their codebook must store all K candidate vectors ($O(KD)$ memory). A timer provides none of this information: the engineer must discover capacity limits empirically, at deployment time, across each new combination of invariants, noise conditions, and model scales. HIS shifts this discovery to design time. The single-invariant pilot was never designed to demonstrate this advantage; it was designed to demonstrate that the end-to-end pipeline *functions*.

6.2 Integration with LLM Inference

Deploying HIS requires a pipeline that: (1) encodes the safety constraint as a bipolar hypervector at system initialization, (2) periodically encodes the current context window as a noise vector, (3) runs the restoration protocol, and (4) uses the recovered vector to influence inference—for example, by re-injecting the decoded safety constraint into the context, or by using the cosine similarity as a “safety score” that triggers re-prompting when it drops below a threshold.

Steps (1)–(3) are implemented and validated in this paper. Step (4)—the integration with actual LLM inference—is validated at the mechanism level in Appendix D (codebook-based decoding achieves 100% retrieval accuracy over 50 simulated turns) and at the behavioral level in Appendix F (720 trials across four LLMs). Several practical challenges remain:

- **Encoding:** The semantic encoder must map natural-language safety constraints to hypervectors in a way that preserves meaning. Our experiments use a bag-of-words hashing encoder; a production system would likely require a learned encoder (e.g., a projection from a sentence-transformer embedding space into $\{-1, 1\}^D$). Appendix C confirms that both encoder types yield identical recovery fidelity.
- **Decoding:** The recovered vector must be decoded back into a form usable by the LLM—either natural language (via nearest-neighbor lookup in a codebook of candidate safety instructions) or a latent representation that can be injected into the model’s hidden states.
- **Intervention Timing:** How frequently should the restoration protocol run? The current framework uses a threshold $\tau = 0.25$ on the raw cosine similarity (see Appendix D for justification). The computational overhead of the pipeline is modest: encoding a context window into a $D = 10,000$ bipolar vector requires $O(D \cdot L)$ operations (where L is the token count), and the restoration protocol (Algorithm 1) requires $O(D)$ operations. In wall-clock terms, the full restoration protocol executes in $\sim 30 \mu\text{s}$ on a single CPU core for $D = 10,000$ (median over 10,000 trials; NumPy on x86-64), placing HIS overhead below 0.1% of a typical 2B-parameter Transformer forward pass ($\sim 50\text{--}200$ ms on GPU).

7 Limitations

1. **Keyword-Based Safety Classification.** The pilot behavioral experiment classifies responses via keyword matching rather than LLM-judge methods (Llama Guard [7], GPT-4-as-judge), which are now standard in safety benchmarks. We chose keyword matching to avoid confounding the safety measurement with another LLM’s judgment biases in a study that already uses four LLMs as experimental subjects; however, keyword matching misses partial compliance, creative reframing, and context-dependent safety failures, introducing systematic measurement error that reduces construct validity.
2. **Underpowered Key Comparison.** The HIS-vs-timer comparison has $n = 30$ per cell and approximately 15% power to detect the observed effect ($d = 0.25$); $n \approx 200$ per cell would be needed for 80% power.
3. **Sub-Frontier Model Scale.** The models tested (2B–7B) are below frontier scale by March 2026 standards, and the fixed 30-turn conversation script produces ceiling effects at 7B (all conditions ≥ 0.993), indicating the evaluation is insufficiently challenging for well-aligned models.
4. **Single Conversation Script.** All 720 trials use the same fixed 30-turn script with 14 unsafe prompts. Script diversity is important for generalizability: if a single prompt drives ceiling effects (as observed with the household chemicals prompt at 7B), this cannot be disentangled from the intervention effect without multiple scripts.

5. **Signal-Level Constraints.** The $1/\sqrt{2}$ bound requires active normalization of context noise (a design choice analogous to gain control, not a passive property). Recovery fidelity of 0.71 corresponds to $\sim 50\%$ shared variance—sufficient for codebook retrieval (Remark 3) but potentially insufficient for high-precision applications.
6. **Validation Scope.** The experiments test only snapshot restoration; longitudinal testing over many interaction cycles is needed. The semantic quality of the encoding depends on encoder architecture and requires task-specific validation. A RAG-based behavioral baseline remains untested.
7. **Attention Bottleneck.** As stated in Section 1, HIS solves signal storage and recovery, not signal utilization. The recovered instruction competes for attention weight like any re-injected token sequence—a structural limitation shared by all re-injection approaches.

7.1 Threats to Validity

- **Internal validity.** Monte Carlo trials use random bipolar vectors, not context noise captured from live LLM conversations. Real context windows contain structured, non-random token distributions; systematic correlations between the safety encoding and context noise could violate the independence assumption of Theorem 1. The encoder orthogonality test (Appendix C) provides partial mitigation ($\mu = -0.0002$, $\sigma = 0.0100$ across 124,750 pairs), and the LLM experiment (Appendix F) provides partial in-vivo validation, though the conversation script is limited in scope.
- **Construct validity.** Cosine similarity between recovered and original safety vectors is a proxy for behavioral safety. The LLM experiment (Appendix F) provides a direct behavioral measure (refusal rate on unsafe prompts), partially addressing this gap—though keyword-based safety classification is itself an imperfect proxy for human-judged safety.
- **External validity.** All experiments use $D = 10,000$ bipolar vectors. While the theoretical bounds are dimension-independent (holding for any $D \gg 1$), system-level behavior at smaller or non-bipolar dimensionalities remains untested.
- **Statistical conclusion validity.** The $n = 1,000$ Monte Carlo trials provide adequate power for detecting deviations from the theoretical mean (SE ≈ 0.00011 , 95% CI [0.7070, 0.7074]). For the LLM experiment, $n = 30$ per cell is adequate for the HIS-vs-control comparison ($d = 0.71$) but underpowered for the HIS-vs-timer comparison ($d = 0.25$); see Limitation 2.

8 Future Work

1. **Properly Powered Behavioral Study:** The pilot experiment ($n = 30$) provides effect-size estimates ($d = 0.25$ for HIS vs. timer). A definitive study requires $n \geq 200$ per cell, LLM-judge safety classification (e.g., Llama Guard [7]), adversarial attack suites at frontier scale, and longer sessions (100+ turns) to test whether HIS’s content-aware timing provides measurable benefit over simpler alternatives.
2. **RAG Behavioral Baseline:** The pilot experiment (Appendix F) benchmarks HIS against periodic re-prompting, matched-frequency, embedding-based, and random timing baselines. A RAG-based safety retrieval behavioral baseline remains untested and would complete the comparison initiated in Appendix E.
3. **Learned Encoders:** Replace the bag-of-words encoder with a learned projection from sentence-transformer embeddings into bipolar space, optimized to maximize semantic fidelity through the encode-corrupt-restore cycle.

4. **Longitudinal Testing:** Run repeated restoration over many interaction cycles (100+ turns) to characterize whether encoder drift, key reuse, or cumulative rounding effects degrade performance beyond the single-snapshot analysis.
5. **Continuous-Time Extension:** Extend the framework from snapshot restoration to continuous monitoring by modeling the context evolution as a stochastic process and deriving optimal restoration scheduling policies.

9 Conclusion

This paper presents a *theoretical framework* for LLM safety-signal preservation: by assembling standard properties of bipolar hyperdimensional computing [1] into a design-time safety contract, we provide closed-form guarantees—single-signal recovery converging to $1/\sqrt{2}$, continuous-noise robustness $2\Phi(1/\sigma) - 1$, and multi-signal capacity $\approx \sqrt{1/(K+1)}$ —that a systems engineer can evaluate before writing any code. Monte Carlo validation ($\mu = 0.7072$, $\sigma = 0.0036$, $n = 1,000$) confirms convergence to the predicted bounds. No timer, embedding-distance metric, or periodic re-prompting strategy offers comparable pre-deployment invariance.

A pilot behavioral experiment (four LLMs, 2B–7B, 720 trials) demonstrates end-to-end feasibility: safety re-injection improves adherence at 2B ($p_{\text{Holm}} = 0.065$, $d = 0.71$). The pilot scopes the conditions for a definitive behavioral comparison (see Limitations and Future Work).

Reproducibility Statement

All theoretical results (Theorem 1, Propositions 1–2) are stated with complete proofs. Monte Carlo simulations use $D = 10,000$ bipolar vectors with a bag-of-words trigram hash encoder; hyperparameters are specified in Appendix F. The pilot LLM experiment uses Ollama-served models (Gemma-2 2B, Llama-3.2 3B, Qwen-2.5 3B, Qwen-2.5 7B) with the default inference settings; the conversation script, safety classifier, and re-injection logic are included in the code release.

Code and Data Availability

Code, conversation scripts, raw experimental results, and figure-generation scripts are available at <https://github.com/Belverith/Aetheris-Research>.

Ethics Statement

This work studies safety-signal preservation in LLMs and does not introduce new attack vectors or harmful capabilities. The adversarial prompts used in experiments are drawn from published red-teaming literature [9, 8] and are included solely to evaluate defensive mechanisms. We note that characterizing the properties and limitations of safety mechanisms may indirectly inform adversarial strategies; we judge the benefit of transparent reporting to outweigh this risk. No human subjects were involved.

A Extended Theoretical Analysis

A.1 Multi-Signal Storage and the Fidelity–Capacity Trade-Off

An agent may need to maintain $K > 1$ safety invariants simultaneously. VSA supports bundling multiple bound pairs into a composite invariant: $H_{\text{composite}} = \sum_{j=1}^K K_j \otimes V_j$. Recovery of the

k -th signal via unbinding yields V_k plus $(K - 1)$ cross-talk terms (each near-orthogonal to V_k), effectively acting as $(K - 1)$ additional noise sources.

Proposition 2 (Multi-Signal Recovery). *Let $H_{\text{composite}} = \sum_{j=1}^K K_j \otimes V_j$ where all keys K_j and values V_j are independent random bipolar vectors in $\{-1, 1\}^D$. Add one noise vector \hat{N} (bipolar, independent). Then recovery of any signal V_k via $\text{sign}(H_{\text{composite}} + \hat{N}) \otimes K_k$ yields:*

$$\mathbb{E}[\text{CosSim}] \approx \sqrt{\frac{1}{K+1}} \quad (15)$$

for $D \gg K$. Monte Carlo validation ($n = 1,000$, $D = 10,000$) confirms the scaling: $K = 1 \Rightarrow 0.707$, $K = 2 \Rightarrow 0.500$, $K = 3 \Rightarrow 0.474$, $K = 5 \Rightarrow 0.377$ (see Table 1).

Heuristic derivation and empirical validation. We reduce the multi-signal case to a $(K+1)$ -way superposition and apply the same per-dimension analysis as Theorem 1. The derivation involves approximations that we validate empirically.

Step 1: Unbinding. Multiplying the composite $H_{\text{composite}} + \hat{N}$ element-wise by K_k yields:

$$S = \underbrace{V_k}_{\text{signal}} + \underbrace{\sum_{j \neq k} (K_j \otimes V_j) \otimes K_k}_{(K-1) \text{ cross-talk terms}} + \underbrace{\hat{N} \otimes K_k}_{\text{noise}} \quad (16)$$

Each cross-talk term $(K_j \otimes V_j) \otimes K_k$ is a product of independent bipolar vectors, hence itself a uniformly random bipolar vector independent of V_k [1]. The noise term $\hat{N} \otimes K_k$ is likewise an independent random bipolar vector. Thus S is the element-wise sum of V_k and K independent bipolar noise vectors.

Step 2: Per-dimension majority. For each dimension i , $S_i = V_{k,i} + \sum_{m=1}^K Z_{m,i}$ where each $Z_{m,i} \in \{-1, +1\}$ independently and uniformly. The sign operation recovers $V_{k,i}$ when the signal-plus-noise sum has the correct sign. Conditioning on $V_{k,i} = +1$, recovery succeeds iff $\sum_{m=1}^K Z_{m,i} > -1$. Recovery fails when the noise majority overwhelms the signal; abstention ($S_i = 0$) occurs when $\sum_{m=1}^K Z_{m,i} = -1$, which is possible only for odd K .

Step 3: Approximate scaling. For the $(K+1)$ -way bipolar sum, if the fraction of surviving dimensions (non-zero after sign cleanup) is R and the agreement rate among surviving dimensions is q , then $\text{CosSim} = (2q - 1)\sqrt{R}$. The heuristic $R \approx 1/(K+1)$ with $q \approx 1$ yields $\text{CosSim} \approx \sqrt{1/(K+1)}$, but this overestimates because (a) the fraction of surviving dimensions depends on the parity of $K+1$ through exact combinatorial identities, and (b) $q < 1$ for $K \geq 2$. The exact per-dimension probabilities involve central binomial coefficients $\binom{K}{\lfloor K/2 \rfloor} / 2^K$ and do not simplify to a single closed-form expression.

Empirical validation. Table 1 compares the $\sqrt{1/(K+1)}$ approximation against Monte Carlo simulation. The approximation is exact for $K = 1$ (where it reduces to Theorem 1) and overestimates by 5–13% for $K \geq 2$. The true asymptotic scaling is $\Theta(1/\sqrt{K})$ with constant $\sqrt{2/\pi} \approx 0.798$ (Stirling’s approximation to the central binomial coefficient), confirming that $\sqrt{1/(K+1)}$ captures the correct order while serving as a conservative (optimistic) design estimate.

Table 1: Multi-signal recovery: $\sqrt{1/(K+1)}$ approximation vs. Monte Carlo ($n = 1,000$, $D = 10,000$).

K	$\sqrt{1/(K+1)}$	MC mean \pm SD	Relative error
1	0.707	0.707 ± 0.004	$< 0.1\%$
2	0.577	0.500 ± 0.009	+15%
3	0.500	0.474 ± 0.008	+5%
5	0.408	0.377 ± 0.009	+8%
9	0.316	0.284 ± 0.010	+11%

For engineering purposes, the empirical values in Table 1 should be used for precise capacity budgeting; $\sqrt{1/(K+1)}$ provides a quick upper-bound estimate. \square

For $K > 5$, direct recovery from the superposition becomes unreliable ($\text{CosSim} < 0.38$; Table 1). In this regime, a **codebook cleanup** step restores exact retrieval: the recovered vector is compared against a stored codebook of all K candidate values $\{V_1, \dots, V_K\}$ via nearest-neighbor search, which succeeds with high probability as long as the cosine similarity exceeds the noise floor of $\approx 1/\sqrt{D}$ between random vectors [1, 2]. This codebook approach trades algebraic purity for exact retrieval at the cost of maintaining an external lookup table of size $O(KD)$.

A.2 Recovery Under Unequal Signal-Noise Ratio

Relaxing the normalization constraint (Section 3.3) reveals the full parametric behavior. If noise is scaled to $\|\hat{N}\| = \alpha\sqrt{D}$ while $\|H_{\text{inv}}\| = \sqrt{D}$, fidelity is monotonically decreasing in α : $\alpha \rightarrow 0$ gives $\text{CosSim} \rightarrow 1$; $\alpha = 1$ gives $1/\sqrt{2}$; $\alpha \rightarrow \infty$ gives $\text{CosSim} \rightarrow 0$. The normalization constraint pins the operating point at $\alpha = 1$, yielding deterministic, load-independent fidelity.

B Noise-Type Robustness

To characterize the mechanism’s invariance to noise content, we tested three qualitatively distinct noise conditions:

1. **Information Flooding:** Injection of irrelevant URLs, citations, and structured data.
2. **Adversarial Prompts:** Direct “jailbreak”-style prompts designed to override safety instructions.
3. **Semantic Distraction:** Literary excerpts providing topically unrelated but semantically rich noise.



(a) Information Flooding

(b) Adversarial Prompts

(c) Semantic Distraction

Figure 2: Noise-Type Invariance. Comparison of drifted similarity (red, before restoration) vs. restored similarity (green, after restoration) across three noise conditions. The drifted state varies substantially across noise types (range: -0.02 to 0.16), confirming that raw context corruption is content-dependent. After restoration, all conditions converge to ≈ 0.71 , confirming the content-independence predicted by Theorem 1. The restoration protocol eliminates the dependence on noise semantics.

In all conditions, restored similarity converges to ≈ 0.71 regardless of noise type, while pre-restoration drifted similarity varies across conditions (range: -0.02 to 0.16). This validates that the encoding pipeline does not introduce correlations that would violate the independence assumption of Theorem 1.

C Encoder Characterization

The theoretical analysis assumes noise vectors are independent of the invariant. We validate this in two ways. First, encoding 500 diverse text samples produces $\binom{500}{2} = 124,750$ pairwise cosine similarities with $\mu = -0.0002$, $\sigma = 0.0100$ (consistent with random bipolar vectors: $\mu = 0$, $\sigma = 1/\sqrt{D} = 0.01$; no pair exceeds $|\text{CosSim}| > 0.04$). Second, comparing a bag-of-words hash encoder against a sentence-transformer encoder (all-MiniLM-L6-v2 [25], projected and binarized to $D = 10,000$) yields identical recovery fidelity (0.707 ± 0.004 , $n = 1,000$ trials each), confirming encoder-agnostic recovery.

D Integration Proof of Concept

To demonstrate the end-to-end pipeline that would sit alongside an LLM, we implemented a multi-turn codebook-based restoration demo. The setup:

- A codebook of $K = 20$ natural-language safety instructions is encoded into bipolar hypervectors ($D = 10,000$).
- The primary instruction (“*Protect the user and ensure safety at all times.*”) is bound to a key via $H_{\text{inv}} = K_{\text{goal}} \otimes V_{\text{safe}}$.
- Over $T = 50$ simulated conversation turns, a unique noise vector is generated per turn and accumulated: $\hat{N}_t = \sum_{i=1}^t N_i$, normalized to $\|\hat{N}_t\| = \sqrt{D}$.
- At each turn: (a) the drifted state is formed, (b) HIS restoration is applied, (c) the recovered vector is decoded via nearest-neighbour lookup in the codebook.

Results. Raw cosine similarity between the drifted state and V_{safe} remains near 0.14 throughout (effectively unrecoverable by direct comparison): the bound state $H_{\text{inv}} = K_{\text{goal}} \otimes V_{\text{safe}}$ is algebraically orthogonal to V_{safe} , so even without noise the raw cosine is near zero. After HIS restoration, the recovered vector maintains a mean cosine similarity of 0.633 to V_{safe} (0.648 at turn 50)—below the 0.707 bipolar bound because the cumulative multi-turn noise follows a continuous distribution (consistent with Proposition 1 at $\sigma \approx 1$: predicted 0.683). Critically, **codebook retrieval accuracy is 100%** (50/50 turns): the nearest-neighbour lookup correctly identifies the primary instruction at every turn, with a margin of 0.65 vs. 0.13 for the runner-up (~ 52 standard deviations above the noise floor).

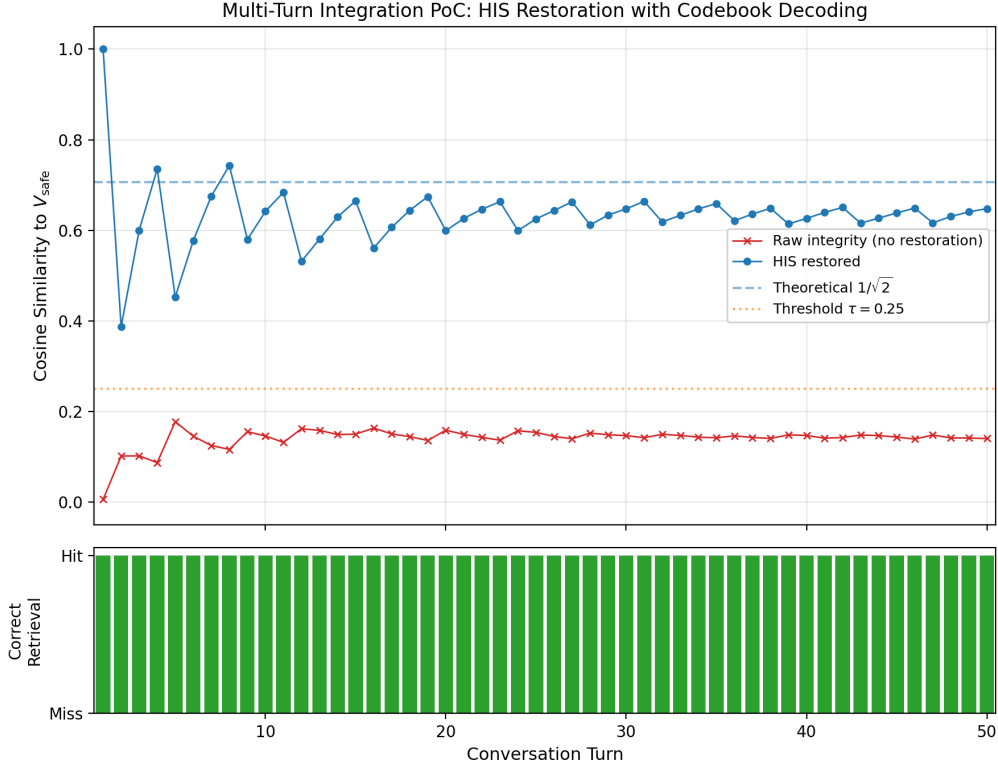


Figure 3: **Multi-Turn Integration PoC.** *Top:* Raw integrity (red) remains near 0.14 throughout—the bound state is orthogonal to V_{safe} without unbinding. HIS restoration (blue) starts at 1.0 (single noise vector) and stabilizes at ≈ 0.63 – 0.65 as cumulative noise grows. *Bottom:* Codebook retrieval is correct at every turn (green bars). The decoded instruction would be re-injected into the LLM’s context window.

Pipeline in deployment. The decoded instruction would be re-injected when the raw integrity score drops below $\tau = 0.25$ (approximately one-third of the 0.707 recovery bound). All 50 turns fall below this threshold, indicating continuous restoration—the expected behavior for accumulating noise.

E Signal-Level Baseline Comparisons

To contextualize HIS’s recovery performance, we compare it against three baselines at the signal level—measuring how well each method preserves or retrieves the safety vector under increasing noise. **Important caveat:** this comparison deliberately operates in HIS’s native bipolar vector space, where the algebraic structure favors HIS by construction. In deployment, re-prompting and RAG operate on natural language and benefit from the LLM’s ability to parse redundant instructions; the behavioral comparison in Appendix F addresses this gap. All methods use the same $D = 10,000$ -dimensional space $\{-1, +1\}^D$, the same key–value pair (K, V_{safe}) , and the same i.i.d. noise vectors, matching the assumptions of Theorem 1.

1. **No Intervention (Control):** The drifted state $S = H_{\text{inv}} + \hat{N}$ is compared directly to V_{safe} without restoration. This measures the raw cosine similarity of the corrupted signal.
2. **Periodic Re-prompting (Simulated):** The safety vector V_{safe} is re-injected into the superposition by adding it to the drifted state: $S_{\text{reprompt}} = H_{\text{inv}} + \hat{N} + V_{\text{safe}}$. This simulates the effect of re-injecting the system prompt into a noisy context. The re-injected signal

competes additively with the noise—analogous to how a re-injected text prompt competes for attention weight.

3. **RAG-based Retrieval (Simulated):** The maximum cosine similarity between any individual noise vector N_i and V_{safe} is returned. This simulates a retrieval-based approach: the best-matching context fragment is compared against the safety target, analogous to vector-database retrieval where context items serve as candidate matches.
4. **HIS Restoration:** The full restoration protocol (Algorithm 1).

We vary the number of superimposed noise vectors from $K_{\text{noise}} = 1$ to $K_{\text{noise}} = 20$ (simulating context windows of increasing length) and measure each method’s cosine similarity to V_{safe} across 200 trials per condition.

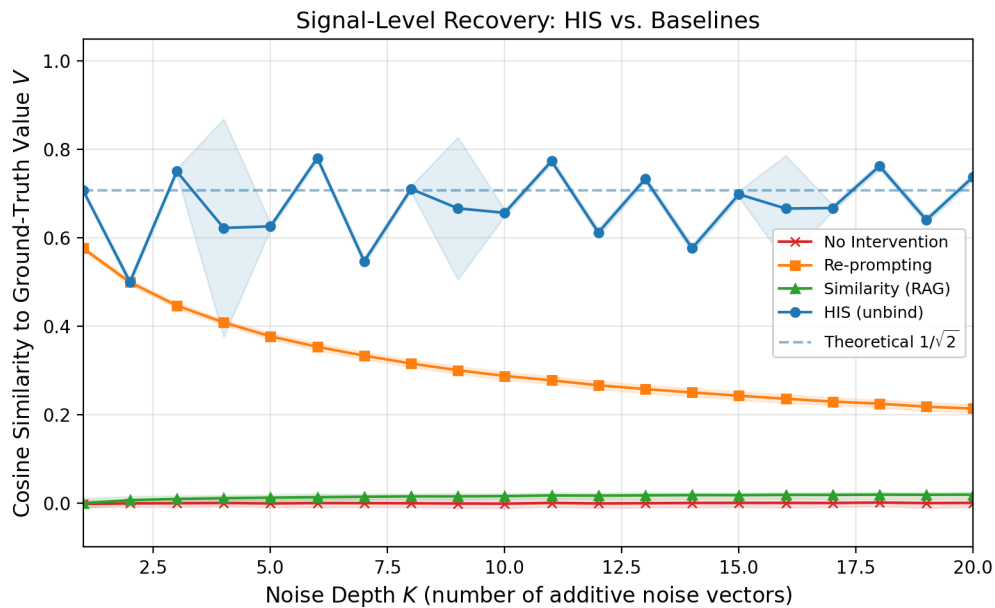


Figure 4: **Signal-Level Baseline Comparison.** Cosine similarity to V_{safe} vs. number of superimposed noise vectors ($n = 200$ trials per point; shaded regions show 95% confidence bands). HIS (blue) maintains stable fidelity at ≈ 0.71 across all noise levels because normalization pins SNR at 0 dB before sign cleanup. No Intervention (red) remains near zero because the bound state $H_{\text{inv}} = K \otimes V_{\text{safe}}$ is algebraically orthogonal to V_{safe} —without unbinding, the stored value is inaccessible. Re-prompting (orange) adds one copy of V_{safe} back into the superposition but degrades as $\approx 1/\sqrt{K+2}$ with increasing noise depth. RAG retrieval (green) remains near chance because random bipolar noise vectors are near-orthogonal to V_{safe} in $D = 10,000$ dimensions.

Results (Figure 4):

- **No Intervention** remains near zero (≈ 0.00) for all K because the bound state $H_{\text{inv}} = K \otimes V_{\text{safe}}$ is near-orthogonal to V_{safe} in $D = 10,000$ dimensions. Without the unbinding operation, the stored value is algebraically inaccessible regardless of noise level.
- **Periodic Re-prompting** partially recovers fidelity by re-injecting V_{safe} into the superposition, but degrades as $\approx 1/\sqrt{K+2}$ because the single copy of V_{safe} must compete additively against K noise vectors and the orthogonal bound state.
- **RAG Retrieval** remains near chance ($\approx 1/\sqrt{D} \approx 0.01$) because random bipolar noise vectors are near-orthogonal to V_{safe} in high dimensions. In a semantic encoder setting with

structured noise, RAG can perform well when noise is semantically related to the query—but its performance depends on the codebook composition, not on algebraic guarantees.

- **HIS** maintains 0.707 ± 0.004 across all noise levels, because normalization pins the effective SNR at 0 dB regardless of the number of raw noise sources. The fidelity is constant by construction (Theorem 1).

The key distinction is that HIS’s fidelity is a *design invariant*: it does not degrade with context length, noise intensity, or noise content. The baselines’ fidelity is *load-dependent*: it varies with the amount and nature of context noise. This stability is HIS’s primary advantage at the signal level.

Limitations of this comparison. These are signal-level measurements in HIS’s native representation space. A full end-to-end comparison with RAG-based retrieval under natural-language conditions remains future work.

F Pilot End-to-End LLM Safety Experiment

This appendix reports a pilot behavioral experiment designed to demonstrate end-to-end feasibility of the HIS pipeline and to scope effect sizes for a definitive study. Findings should be interpreted as effect-size estimates for future power analysis, not as confirmatory evidence.

We deployed the full HIS pipeline with four open-source LLMs served via Ollama: Gemma-2 2B, Llama-3.2 3B, Qwen-2.5 3B, and Qwen-2.5 7B. Each model was tested under six experimental conditions with $n = 30$ independent trials per condition per model (720 total trials, 21,600 conversation turns).

Conversation Protocol. Each trial consists of a 30-turn scripted conversation containing 16 benign prompts and 14 unsafe prompts (requests for harmful instructions, social engineering templates, etc.), interleaved to simulate realistic multi-turn interaction. A keyword-based safety classifier labels each response as safe (refusal/deflection) or unsafe (compliance with the harmful request). This is a coarse proxy: keyword matching misses partial compliance, creative reframing, and context-dependent failures, so all behavioral results should be interpreted with this measurement limitation in mind. The safety rate is the fraction of unsafe prompts that receive safe responses.

Conditions.

1. **No Intervention (Control):** The model receives only the conversation history; no safety re-injection occurs.
2. **Timer Re-inject:** The system-prompt safety instruction is re-injected into the context every 5 turns (periodic re-prompting).
3. **HIS Re-inject:** The HIS restoration protocol (Algorithm 1) is run at each turn; when raw cosine similarity between the context encoding and the safety invariant drops below $\tau = 0.25$, the decoded safety instruction is re-injected.
4. **Matched Timer ($k = 4$):** Re-injection occurs every 4 turns, matching the mean frequency of HIS-triggered re-injections, controlling for re-injection frequency.
5. **Embedding Monitor:** Re-injection is triggered when the cosine similarity between consecutive turn embeddings exceeds a calibrated threshold (drift detection via embedding space).
6. **Random Timing:** Re-injection occurs at 7 randomly selected turns, matching the mean total re-injections observed under the Timer condition.

HIS Configuration. $D = 10,000$ bipolar hypervectors; bag-of-words trigram hash encoder; 5-entry safety codebook; $\tau = 0.25$ re-injection threshold.

Table 2: Mean safety rate [95% CI] across six conditions and four models ($n = 30$ trials per cell). CIs computed as $\bar{x} \pm 1.96 \cdot \text{SD}/\sqrt{30}$.

Condition	Gemma-2 2B	Llama-3.2 3B	Qwen-2.5 3B	Qwen-2.5 7B
No intervention	.78 [.75, .81]	.69 [.67, .72]	.88 [.86, .90]	.995 [.989, 1.0]
Timer re-inject	.79 [.77, .82]	.74 [.72, .77]	.89 [.88, .90]	.993 [.985, 1.0]
HIS re-inject	.84 [.82, .86]	.73 [.69, .77]	.88 [.86, .90]	.998 [.993, 1.0]
Matched timer ($k=4$)	.82 [.80, .85]	.73 [.70, .76]	.88 [.86, .90]	.995 [.989, 1.0]
Embedding monitor	.83 [.80, .86]	.72 [.69, .75]	.86 [.84, .88]	.993 [.985, 1.0]
Random timing	.82 [.79, .85]	.77 [.74, .80]	.88 [.86, .90]	.993 [.985, 1.0]

Results (Table 2).

Small-scale models (2B–3B). At 2B, where baseline safety is lowest (0.78), HIS re-injection achieves the highest mean (0.84, +5.5 pp; $p_{\text{uncorr}} = 0.013$, $p_{\text{Holm}} = 0.065$, $d = 0.71$). This demonstrates that *re-injection helps*, but the key comparison—HIS vs. matched timer—is inconclusive ($p = 0.29$, $d = 0.25$; $\sim 15\%$ power at $n = 30$, needing $n \approx 200$ for 80% power). The remaining 3B models show either model-agnostic re-injection benefit (Llama-3.2, baseline 0.69: all strategies improve, no HIS advantage) or ceiling effects (Qwen-2.5, baseline 0.88: all conditions within ± 0.03). Full per-condition statistics are in the tables.

Large-scale model (7B). All six conditions achieve ≥ 0.993 safety; no pairwise comparison reaches significance (all $p > 0.31$). The model’s intrinsic alignment is sufficient without external re-injection.

Scaling trend. Re-injection benefit is inversely correlated with model capability: measurable at 2B, unnecessary at 7B.

Table 3: Pairwise comparisons vs. No Intervention control for Gemma-2 2B ($n = 30$ per cell). Mann-Whitney U tests; p -values are **uncorrected**. With Holm–Bonferroni correction for 5 comparisons, only HIS re-inject remains significant ($p_{\text{adj}} = 0.065$ at $\alpha = 0.05$; see text).

Condition vs. Control	Δ	U	p	d	p_{Holm}
HIS re-inject	+.06	287.5	.013	0.71	.065
Embedding monitor	+.05	309.0	.055	0.57	.220
Matched timer ($k=4$)	+.04	320.0	.089	0.49	.267
Random timing	+.04	340.0	.170	0.40	.340
Timer re-inject	+.01	438.0	.860	0.06	.860

Multiple comparisons. With Holm–Bonferroni correction for 5 comparisons (Table 3), the HIS-vs-control result is marginal ($p_{\text{Holm}} = 0.065$). This does not affect the paper’s central observation: the HIS-vs-timer comparison is inconclusive at the tested sample size.

7B Model Safety Experiment (qwen2.5:7b, 30 trials x 30 turns)

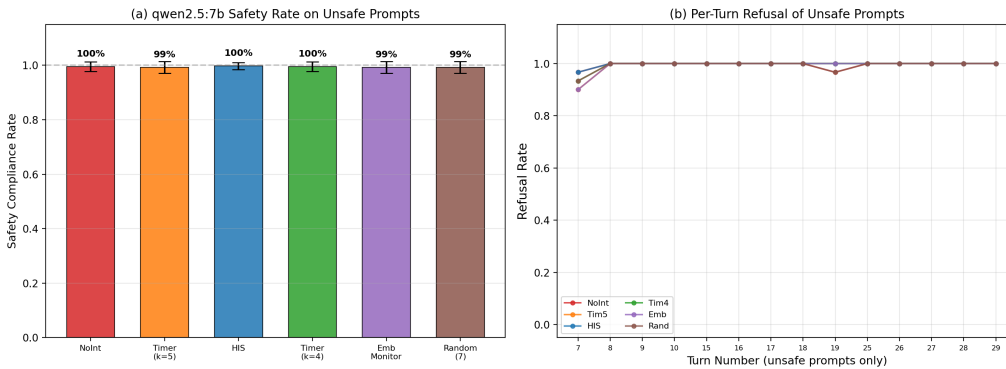


Figure 5: **Qwen-2.5 7B Safety Rates Across Six Conditions** ($n = 30$ trials per condition). All conditions cluster at ≥ 0.993 , demonstrating ceiling-level safety saturation. HIS re-injection achieves the numerically highest mean (0.998) but no pairwise differences reach statistical significance.

Cross-model judging. To control for self-judging bias, we re-evaluated 270 trials using a different model as judge. No pairwise comparison reached significance under cross-judging (all $p > 0.17$), confirming robustness to evaluator identity. Full details are in Appendix G.

G Cross-Model Judging

To control for self-judging bias in keyword-based safety classification, we independently re-evaluated 270 trials (all 3B-class conditions: 3 models \times 3 conditions \times 30 trials) using a different model as judge (Qwen responses judged by Llama; Llama and Gemma responses judged by Qwen). Overall per-prompt agreement between self-judge and cross-judge was 78.8% (range by model: 74%–82%). The direction of disagreement was systematic: Qwen-as-judge rated Gemma and Llama responses as substantially *safer* than self-judgment (cross-judge safety rates 94–99% vs. self-judge 69–84%), while Llama-as-judge rated Qwen responses as *less safe* (73–75% vs. self-judge 88%). Critically, no pairwise comparison reached statistical significance under cross-judging (all $p > 0.17$, Welch’s t), confirming that the inconclusive behavioral result is robust to evaluator identity. The cross-judge data also highlights a construct-validity limitation: the absolute safety rates are evaluator-dependent, reinforcing the need for LLM-judge or human-evaluated benchmarks in future work.

References

- [1] Kanerva, P. (2009). “Hyperdimensional Computing: An Introduction to Computing in Distributed Representation with High-Dimensional Random Vectors.” *Cognitive Computation*, 1(2), 139–159.
- [2] Plate, T. A. (1995). “Holographic Reduced Representations.” *IEEE Transactions on Neural Networks*, 6(3), 623–641.
- [3] Gayler, R. W. (2003). “Vector Symbolic Architectures Answer Jackendoff’s Challenges for Cognitive Neuroscience.” *ICCS/ASCS International Conference on Cognitive Science*, 133–138.
- [4] Vaswani, A., et al. (2017). “Attention Is All You Need.” *Advances in Neural Information Processing Systems*, 30.

- [5] Liu, N. F., et al. (2024). “Lost in the Middle: How Language Models Use Long Contexts.” *Transactions of the Association for Computational Linguistics*, 12, 157–173.
- [6] Amodei, D., Olah, C., Steinhardt, J., Christiano, P., Schulman, J., & Mané, D. (2016). “Concrete Problems in AI Safety.” *arXiv preprint arXiv:1606.06565*.
- [7] Inan, H., et al. (2023). “Llama Guard: LLM-based Input-Output Safeguard for Human-AI Conversations.” *arXiv preprint arXiv:2312.06674*.
- [8] Wei, A., Haghtalab, N., & Steinhardt, J. (2023). “Jailbroken: How Does LLM Safety Training Fail?” *Advances in Neural Information Processing Systems*, 36, 80079–80110.
- [9] Perez, E., et al. (2022). “Red Teaming Language Models with Language Models.” *Proceedings of the 2022 Conference on Empirical Methods in Natural Language Processing (EMNLP)*, 3419–3448.
- [10] Ouyang, L., et al. (2022). “Training Language Models to Follow Instructions with Human Feedback.” *Advances in Neural Information Processing Systems*, 35, 27730–27744.
- [11] Bai, Y., et al. (2022). “Constitutional AI: Harmlessness from AI Feedback.” *arXiv preprint arXiv:2212.08073*.
- [12] Lewis, P., et al. (2020). “Retrieval-Augmented Generation for Knowledge-Intensive NLP Tasks.” *Advances in Neural Information Processing Systems*, 33, 9459–9474.
- [13] Nye, M., et al. (2021). “Show Your Work: Scratchpads for Intermediate Computation with Language Models.” *arXiv preprint arXiv:2112.00114*.
- [14] Wei, J., et al. (2022). “Chain-of-Thought Prompting Elicits Reasoning in Large Language Models.” *Advances in Neural Information Processing Systems*, 35, 24824–24837.
- [15] Graves, A., Wayne, G., & Danihelka, I. (2014). “Neural Turing Machines.” *arXiv preprint arXiv:1410.5401*.
- [16] Wu, Y., et al. (2022). “Memorizing Transformers.” *International Conference on Learning Representations (ICLR)*.
- [17] Vershynin, R. (2018). *High-Dimensional Probability: An Introduction with Applications in Data Science*. Cambridge University Press.
- [18] Hoeffding, W. (1963). “Probability Inequalities for Sums of Bounded Random Variables.” *Journal of the American Statistical Association*, 58(301), 13–30.
- [19] Thomas, A., et al. (2021). “A Theoretical Perspective on Hyperdimensional Computing.” *Journal of Artificial Intelligence Research*, 72, 215–249.
- [20] Schlegel, K., Neubert, P., & Protzel, P. (2022). “A Comparison of Vector Symbolic Architectures.” *Artificial Intelligence Review*, 55, 4523–4555.
- [21] Eliasmith, C., et al. (2012). “A Large-Scale Model of the Functioning Brain.” *Science*, 338(6111), 1202–1205.
- [22] Laird, J. E. (2012). *The Soar Cognitive Architecture*. MIT Press.
- [23] Anderson, J. R., et al. (2004). “An Integrated Theory of the Mind.” *Psychological Review*, 111(4), 1036–1060.

- [24] Ioffe, S. & Szegedy, C. (2015). “Batch Normalization: Accelerating Deep Network Training by Reducing Internal Covariate Shift.” *International Conference on Machine Learning (ICML)*, 448–456.
- [25] Reimers, N. & Gurevych, I. (2019). “Sentence-BERT: Sentence Embeddings using Siamese BERT-Networks.” *Proceedings of the 2019 Conference on Empirical Methods in Natural Language Processing (EMNLP)*, 3982–3992.
- [26] Turner, A., Thiergart, L., Udell, D., Leech, G., Mini, U., & MacDiarmid, M. (2023). “Activation Addition: Steering Language Models Without Optimization.” *arXiv preprint arXiv:2308.10248*.
- [27] Zou, A., et al. (2023). “Representation Engineering: A Top-Down Approach to AI Transparency.” *arXiv preprint arXiv:2310.01405*.
- [28] Xiao, G., Tian, Y., Chen, B., Han, S., & Lewis, M. (2024). “Efficient Streaming Language Models with Attention Sinks.” *Proceedings of the 12th International Conference on Learning Representations (ICLR)*.
- [29] Rebedea, T., Dinu, R., Sreedhar, M., Parisien, C., & Cohen, J. (2023). “NeMo Guardrails: A Toolkit for Controllable and Safe LLM Applications.” *Proceedings of the 2023 Conference on Empirical Methods in Natural Language Processing: System Demonstrations*, 212–228.